SDSS'Rio 2010 STABILITY AND DUCTILITY OF STEEL STRUCTURES
E. Batista, P. Vellasco, L. de Lima (Eds.)
Rio de Janeiro, Brazil, September 8 - 10, 2010

STRENGTH AND DUCTILITY OF STEEL BEAMS WITH FLANGE HOLES

K.S. Sivakumaran, P. Arasaratnam, and M. Tait

Department of Civil Engineering, McMaster University, Hamilton, ON, CANADA, L8S 4L7
e-mail: siva@mcmaster.ca

Key words: Experimental, Steel beams, Flange holes, Ductility, Steel standards

Abstract: *This paper presents an experimental investigation, involving twenty five steel beam specimens, on the effects of flange holes on the flexural behaviour of steel I-beams. This study used ASTM A992 grade steel beams. Circular holes of various diameters, ranging form 0% to 48% of the gross flange area are under consideration Based on the experimental results, this research study recommends a design approach analogous to the axial tension member provisions as per the current CAN/CSA-S16.01 standard [1]. The comparison of the proposed procedure with the 15% exemption rule as per current steel standard S16.01 [1] demonstrated that the current code provision is unnecessarily conservative for steel grades such as A992 steel. On the other hand, the current code provision may not be adequate for higher strength steels such as HSLA 80 steel, ASTM A913 Gr: 60 and HPS-485W having the minimum yield-to-ultimate strength ratio of more than 0.85.*

1 INTRODUCTION

Flange holes are frequently made in structural steel construction, primarily for bolting purposes. The influence of flange holes on the flexural behaviour of beam members has been the focus of debate for many years. Early North American design codes allowed a designer to place holes in flanges up to 15% of the gross area of the tension flange without penalty. If more than 15% of the gross flange area is removed, the amount of area exceeding 15% would be deducted in calculating the section properties and typically, only the yield moment could be used rather than the plastic moment. This provision was based on the study by Lilly and Carpenter [2] on riveted plate girders made of ASTM A7 steel having the yield-to-ultimate strength (F_y/F_u) ratio of about 0.5. However, in 1989, the Allowable Stress Design version of specification [3] adopted a new provision that altered the use of the 15% exemption rule in this subject matter. This specification introduced for the first time a mathematical formula based on the ratio of the fracture strength of net area ($A_{fn}F_u$) and the yield strength of gross area ($A_{fg}F_y$) of the tension flange to ignore the effects of holes. The present AISC-Load and Resistance Factor Design version [4] of the specification also follows the same procedure as specified in the 1989-AISC specification [3] to ignore the effect of flange holes.

The present trend in steel construction industry is to use higher strength steels with better structural performance over traditionally used ASTM A36 steel. These high strength steels have the specified yield-to-ultimate strength ratio ranging from 0.75 to a code permitted maximum of 0.85. In some instances, steels such as HPS-485W, HSLA 80 steel and ASTM A913 Gr: 60 exhibit yield-to-ultimate strength values of more than 0.85[5]. Nevertheless, the comparisons of corresponding various international code provisions indicate that the 15% exemption rule which is currently in use as per the clause 14.1 of the current Canadian Steel Design Code [1] is more restrictive for steel grades having the yield-to-ultimate strength of less than 0.85, whereas it is inadequate and inappropriate for the high strength steels with the minimum yield-to-ultimate strength of more than 0.85.

2 THE RESEARCH PROGRAM

The objectives of the research program presented in this paper were: (i) to investigate the effects of flange holes and flange fastener holes on the strength and rotation capacity of steel I-beams made of ASTM A992 steel, (ii) to assess the applicability of the 15% exemption rule used in the clause 14.1 of the current steel code provision [1] along with various other international steel code provisions dealing with the proportioning of flexural members with flange holes (or fastener holes) and (iii) to provided recommendations on the modification of the current CSA code provision[1].

2.1 Test Specimens

The test program considered twenty five full scale beam specimens (Beam section W200X42) each having a nominal length of 3050 mm. All beam specimens were from the same production batch thus the material characteristics discrepancy would be minimal. The tests were divided into four series as follows:

Series-1: This series involved the beam tests with solid flanges. Four beams under consideration were named as A100-1, A100-2, A100-3 and A100-4, wherein 'A100' denotes that the area of tension flange of 100% and the number that follows denotes the test-number.

Series-2: The beam tests of this series contain holes in tension flanges only. Seven different configurations with the net flange area-to-gross flange area (A_{fn}/A_{fg}) ratio between 90% and 50% were considered. The beam specimens tested in this category were named as A90-1, A85-1, A80-1, A75-1, A70-1, A60-1 and A50-1. For example, here, A70 indicates that (A_{fn}/A_{fg}) ratio is 70%. In addition, tests on the beam specimens A75, A70 and A60 were repeated due to the fact that such beam specimens exhibited dominant failure modes varying from a mixed type of local compression flange buckle followed by net-section fracture to a definite net-section fracture.

Series-3: This series included beam specimens with holes in both tension and compression flanges. It includes four tests A85-B-1, A75-B-1, A70-B-1 and A60-B-1, where 'B' denotes both flanges. The purpose of this test was to investigate the flexural behaviour when holes exist in both flanges.

Series-4: This series included beam specimens with flange holes in both flanges, and with fasteners placed in these holes. Standard size of high strength ASTM A490 fasteners, leaving a clearance of approximately 2 mm between the perimeter of hole and the outer surface of the fastener were inserted into the holes of beam specimens: A85-F-1, A75-F-1, A70-F-1 and A60-F-1, where "F" represents fasteners. The fasteners were tightened by a hand wrench to a specific level. The purpose of this type test was to investigate the role of fasteners in resisting the flexural stresses in compression flanges.

2.1.1 Mechanical Characteristics

Six standard tension coupon tests involving 3-flange coupons and 3-web coupons were conducted. All coupons, except the web coupons obtained closer to the flange-web junction, exhibited a sharp yield point followed by a yield plateau. However, the web coupons obtained closer to the flange-web junction exhibited no sharp yield point, and showed higher yield and ultimate strengths, and lower ductility compared to other tension coupons tested in this research program. This can be attributed to the fact that higher stresses exerted at the corner of rolled sections during the course of rolling process and faster cooling following rolling due to the smaller web thickness. The average measured elastic modulus of such coupons was of 215GPa. The yield strength of each coupon was established by the method of 0.2% strain offset, though the flange and middle-web coupons exhibited a shaper yield point. The average measured yield and ultimate strength of flange coupons were of 409 MPa and 531 MPa, respectively resulting in the yield-to-ultimate strength ratio of 0.77.

2.2 Testing of Beams

Test Setup: Figure 1 shows a photographic image of the overall test setup. Each beam specimen was simply supported at its ends and was subjected to two point loads applied at a distance of 750 mm apart leaving a shear span of approximately 1075 mm on either side of the mid-span of the test beam. The test arrangements allowed for large end rotations and vertical displacements that might occur during the test.

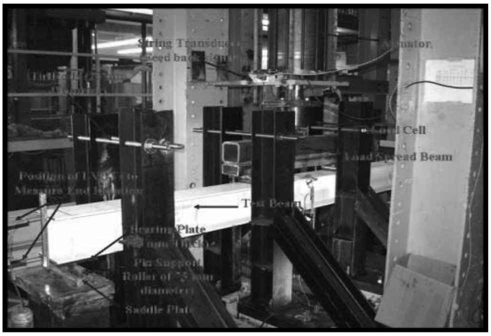

Figure 1: Overall View of Test Setup

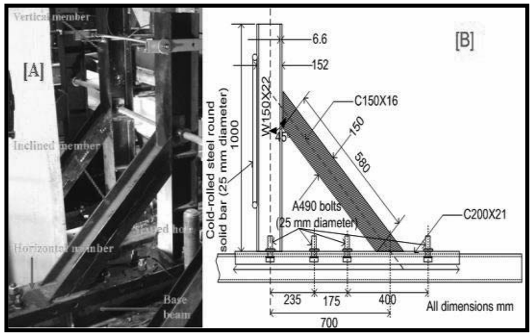

Figure 2: Bracing System

Bracing System: Figure 2 shows a close-up view of the bracing system used in this test program. The triangular bracing system consisted of 3 members whose sizes are shown. A solid cold-rolled bar of 25 mm diameter was welded to the vertical member to function as a knife edge guide. The whole assembly was firmly fastened to the laboratory test floor. Prior to applying the test load, the bracing frames were adjusted such as to touch the flange tips of the test specimen and then tightened to the test floor.

Loading System: As could be seen in Figure 1, the loading system consisted of a 500 mm stroke actuator combined with a commercially available load cell of 900 kN capacity and a 500 mm stroke string transducer attached between the load cell and the outer perimeter of the actuator. Since this is a displacement controlled loading system, it also included a controller, function generator, power supply and a servo valve. The loading system was positioned upside down and loaded from above at mid-span.

Instrumentation: In order to determine the rotation of the beam specimen, potentiometers were placed at each ends of the beam. The differential readings between a pair of potentiometers and a pair of LVDTs and the corresponding vertical distances between them were used to calculate the beam end rotations. The deferential reading between a pair of vertical potentiometers and the corresponding horizontal distances between them were used to establish the rotations at load points. The mid-span deflection of the test beam was measured using potentiometer S.P-3. The vertical deflections at the quarter points of the test beams were also measured using potentiometers. High elongation capacity strain gages were also used in some of the beam tests. Additional instruments such as LVDT-3 and LVDT-4 were used to monitor the out-of-plane movements of the compression flanges with respect to the tension flange at the center of the mid-span. These instruments detected the initiation of local buckling at the center span of the test beam.

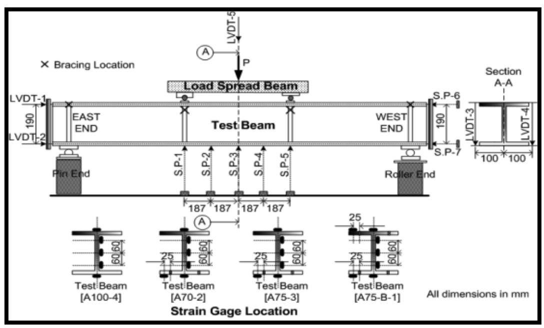

Figure 3: Instrumentation of Test Beam

Test Procedure: Once the instruments were properly attached to the specimen, it was preloaded using the displacement control loading system. The applied preloading was within the elastic range. The beam specimen was then unloaded and instruments were reset. Once this preload protocol is completed, which was to ensure proper seating of the test beam within the loading frame, actual loading began. The test beams were subjected to increasing displacements until failure. The loading rate of 0.025 mm/sec was maintained throughout the test. The beam test was considered complete when the load versus mid-span deflection curve reached below the plastic load again on the unloading branch. However, in the case of beam tests where the failure of the specimen occurred as a result of net-section fracture the test was terminated as soon as a sudden drop in loading was noticed.

3 TEST RESULTS

Some of the results reported herein include normalized quantities of (1) load versus mid-span deflection, (2) moment versus load point rotation and (3) moment versus beam end rotation. The rotation is the average of the rotations measured underneath the two load points. Table 1 presents the measured peak moments M_m associated with each test and the theoretical gross-section plastic moment M_P of each test specimen. Theoretical M_P considers the openings and the resulting neutral axis shift. Table 1 also provides the percentage reduction in strength as compared to the solid beams (see column 7).

Table 1: Comparison of Experimental Peak Moments with Theoretical Plastic Gross-Section Moment

Type of Test (1)	**Beam ID** (2)	**[A_{fn}/A_{fg}] (%)** (3)	**[$A_{fn}F_u$/ $A_{fg}F_y$]** (4)	**M_m (Test) (kNm)** (5)	**M_{ave} (Test) (kNm)** (6)	**%difference compared to solid section** (7)	**M_{Pave} (kNm)** (8)	**Average M_m/ M_P** (9)
Series-1	**A100-1**	100	**1.30**	215	214	0.0	176	1.22
	A100-2	100	**1.30**	214				
	A100-3	100	**1.30**	214				
	A100-4	100	**1.30**	214				
Series-2	**A90-1**	91	**1.18**	214	214	0.0	176	1.22
	A85-1	85	**1.10**	216	216	0.9	176	1.23
	A80-1	79	**1.03**	212	212	0.9	174	1.22
	A75-1	74	0.96	210	209	2.3	175	1.19
	A70-1	71	0.92	204	204	4.7	176	1.16
	A60-1	62	0.81	197	195	8.9	174	1.12
	A50-1	52	0.67	178	178	16.8	172	1.03
Series-3	**A85-B-1**	86	**1.17**	210	210	1.8	178	1.18
	A75-B-1	74	0.96	200	200	6.5	176	1.14
	A70-B-1	70	0.91	197	197	7.9	176	1.12
	A60-B-1	63	0.82	192	192	10.3	179	1.07
Series-4	**A85-F-1**	85	**1.10**	212	212	0.9	175	1.21
	A75-F-1	74	0.96	210	210	1.9	174	1.21
	A70-F-1	70	0.91	207	207	3.3	177	1.17
	A60-F-1	62	0.81	194	194	9.3	175	1.10

Series-1: Solid Beam Tests: The maximum moment carrying capacity of solid beams A100-1, A100-2, A100-3 and A100-4 were 215 kN.m, 214 kN.m, 214 kN.m and 214 kN.m, respectively. However, the corresponding measured average load point rotations corresponding to peak moment were of 0.0938, 0.0972, 0.0949 and 0.0878 radians, respectively, resulting in the maximum deviation from the average measured rotation (0.0934 radians) of approximately 6%. The normalized moment (M/M_P) versus the normalized load point rotation (Θ/Θ_P) relationship for each solid beam was established. The moment versus load point rotation relationship was in close agreement up to the peak moment, even though slight variations were observed perhaps due to the inherent variability associated with the presence of residual stresses and initial geometric imperfections. Two different rotation capacities such as R_y (a measure of available rotation capacity corresponding to the plastic moment M_P obtained on the unloading branch) and R_m (rotation capacity at peak moment) were established in this research program. The average measured R_y and R_m of the solid beam specimens were 23.5 and 13.1, respectively. The failure of the solid beam was due to local flange buckling of the compression flange which was followed by lateral torsional buckling in the critical span region.

Series-2: Beams Having Holes in Tension Flange Only: Figure 4 shows the normalized moment, M/M_P versus the normalized average load point rotation, Θ/Θ_P for the beam specimens with holes in tension flanges only. In order to illustrate how the flexural behaviour of steel member could be influenced due to the presence of holes in the tension flanges, the moment-rotation response of a solid beam (A100-3) is also shown in the same figure. Figure 5 shows a close up view of failure pattern of the beam specimen (A60-3) failed as a result of net-section fracture through the holes in tension flange.

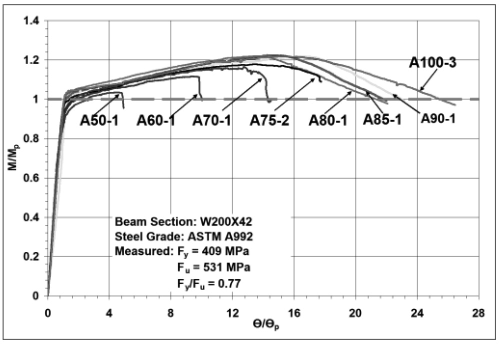

Figure 4: Normalized Moment Versus Normalized Load Point Rotation

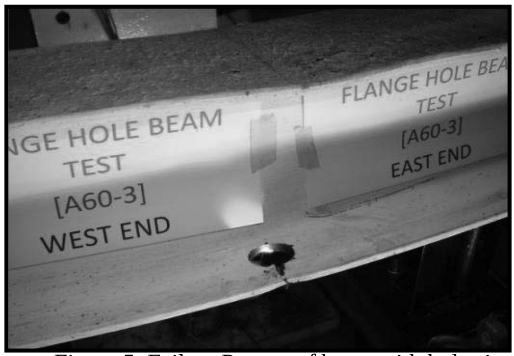

Figure 5: Failure Pattern of beam with holes in Tension Flange

From figure 4, it can be noted that the rotation capacities of the flexural members were reduced even when the holes removed was small, say approximately 10% (A90-1). However, it can be observed that the strength of the flexural members was not significantly impacted provided the nominal net-section fracture strength was greater than nominal gross-section yield strength ($A_{fn}F_u \geq A_{fg}F_y$). This ratio is given in Table 1- Column 4. The percentage reduction in strength (Table 1- Column 7) increased as the $A_{fn}F_u/A_{fg}F_y$ ratio became lower than 1.0. Thus, for beam specimens having the $A_{fn}F_u/A_{fg}F_y$ ratio of 0.96 (26% flange holes of gross flange area) and 0.92 (29% flange holes of gross flange area), the percentage reductions in the average maximum load were of 2.3% and 4.7%, respectively, compared to that of solid beams. These specimens having the $A_{fn}F_u/A_{fg}F_y$ of 0.96 and 0.92 eventually failed by net section fracture which occurred after visible local bulking of the compression flanges in the uniform moment region which can be seen in Figure 5. However, for beam specimens having the $A_{fn}F_u/A_{fg}F_y$ ratio of 0.81 (38% holes of gross flange area) and 0.68 (48% holes of gross flange area), which were well below 1.0, the percentage reductions in the average maximum applied load were of 8.9% and 16.8%, respectively. Such beam specimens failed by net-section fracture, prior to local bucking of compression flange. The reduction in the moment capacity of beam specimens, having the $A_{fn}F_u/A_{fg}F_y>1.0$, was not substantial, although a slight reduction did occur with increasing hole size. Based on these results, suppose it is presumed that any strength reductions within ±5% range can be ignored from a design stand point, then the tension flange holes of up to 29% of the gross flange area can be safely ignored in beams made of ASTM A992 steel having yield-to-ultimate strength ratio of 0.77. Table 1- Column 9 gives the ratio of test moment to theoretical moment resistance. For series-2 specimens, since the M_m/M_P for all specimens were more than 1.0, it can be concluded that the tension flange rupture did not occur prior to the attainment of the gross-section plastic moment, when the holes removed was from 9% to 48%.

Series-3: Beam Having Holes in Both Flanges: As presented in Table 1, the percentage decrease in the moment capacity of beam specimens with holes in both flanges (Series-3) having the $A_{fn}F_u/A_{fg}F_y$ ratio of 1.17, 0.96, 0.91 and 0.82, compared to the solid beams, were 1.8%, 6.5%, 7.9% and 10.3%, respectively. As expected, the flexural behaviour of beam specimens in terms of strength and rotation capacity was considerably influenced as holes were present in both flanges. The percentage decrease in the maximum moment capacity of beam specimens having the $A_{fn}F_u/A_{fg}F_y$ ratio of 1.17 (A85-B-1), 0.96 (A75-B-1), 0.91 (A70-B-1) and 0.82 (A60-B-1), compared to the corresponding beam specimens having holes in the tension flanges only (Series-2) were of 2.7%, 4.2%, 3.2% and 1.4%, respectively. The beam specimen having the $A_{fn}F_u/A_{fg}F_y$ ratio of 0.96 (26% holes of gross flange area), which is closer to 1.0, failed due to local buckling of the compression flange whereas, similar beam specimen ($A_{fn}F_u/A_{fg}F_y$ =0.96) having holes in the tension flange only failed due to net-section fracture of the tension flange, which occurred after noticeable local buckling of the compression flange. This can be attributed to the fact that the compression flange was weakened locally due to the presence of holes which resulted in early yielding of the locally buckled compression flange. However, the beam specimens having the $A_{fn}F_u/A_{fg}F_y$ ratio of 0.91 and 0.82 failed due to tension fracture.

Series-4: Beam Tests Having Holes With Fasteners in Both Flanges: These tests were somewhat similar to Series-3 tests, in that both set of beams had holes in both flanges, except that fasteners were present in the holes in the current set of beams. For beam specimens having the $A_{fn}F_u/A_{fg}F_y$ ratio of 1.10 (A85-F-1), 0.96 (A75-F-1), 0.91(A70-F-1) and 0.82 (A60-F-1), the percentage reduction in the maximum moment capacity in compared to similar solid beam specimens, were of 0.9%, 1.9%, 3.3% and 10.3%, respectively. The moment capacities of beam specimens were greatly improved when the holes in the compression flanges were filled with the standard size of fasteners. The percentage improvement in the maximum moment capacity of beam specimens having the $A_{fn}F_u/A_{fg}F_y$ ratio of 1.10, 0.96, 0.91 and 0.81 when compared to the similar beam sections having holes in both flanges were of approximately 50%, 71%, 58%, and 10%, respectively. This clearly indicated that the presence of fasteners within the holes in the compression flanges improved the moment resistance of beams with flange holes.

4 PROPOSED DESIGN APPROACH

Largest experimentally measured moment (M_m), the calculated gross-section plastic moment ($M_P= Z_gF_y$) and the calculated net-section fracture moment ($M_{fn}= Z_nF_u$) of each beam specimens were established. Note that in calculating the plastic section modulus of net-section, Z_n, the neutral axis of the net-section was presumed to be shifting from the neutral axis of the gross-section to that of the net-section for beam specimens having holes in tension flanges only. Also, similar procedure was adopted for beam specimens having the fastener holes in both flanges although, the strain measurements at the middle of the web indicated that the movement of the neutral axis was not detected. Nevertheless, the consideration of the position of neutral axis shifting from the gross-section to net-section would yield a lower moment capacity [conservative design approach]. Comparing the gross-section plastic moment (M_P) and the net-section fracture moment (M_{fn}), the M_P/M_{fn} ratio increased with increasing $A_{fn}F_u/A_{fg}F_y$ ratios. This suggested the proposed design approach which is analogous to an axial tension member provision. That is the gross-section plastic moment capacity and net-section fracture moment should be checked and the lesser of two could be used as a design moment.

However, a detail analysis of the experimental results [Not given here] indicated that the (M_P/M_{fn}) ratio was less than 0.85 when the $A_{fn}F_u/A_{fg}F_y$ ratio was greater than 1.0 for beam specimens having holes in either tension flanges only or fastener holes in both flanges. Moreover, in such cases, the beam specimens eventually failed due to local buckling of the compression flange preceded by lateral torsion buckling in the critical span region [ductile failure]. On the other hand, the M_P/M_{fn} ratio was greater than 0.85 when the $A_{fn}F_u/A_{fg}F_y$ ratio was reduced to below 1.0. The failure of beam specimens in this case was mainly due to local buckling of the compression flange in the critical span (mid-span) region which was eventually followed by net-section fracture in the tension flange [brittle failure]. However, for the beam specimens having holes in both flanges and having the $A_{fn}F_u/A_{fg}F_y$ ratio of greater than 0.95, the M_P/M_{fn}

ratio was less than 1.0. Also, the failure of beam specimens in such cases was mainly due to local buckling of the compression flange preceded by lateral torsional buckling in the critical span. On the other hand, as the $A_{fn}F_u/A_{fg}F_y$ ratio became less than 0.95 the M_P/M_{fn} ratio was increased to more than 1.0. The failure of beam specimens in such cases was mainly due to net-section fracture of the tension flange. By considering all the scenarios tested in this research program, a factor of 0.85 can be considered as an optimum upper bound that should be used to multiply the theoretical net-section fracture moment (M_{fn}). Therefore, this research study suggests a design check, which is analogous to the tension member provision as per the current CAN/CSA-S16.01 [1] standard,; (a) The gross-section shall be designed for the gross-section plastic moment capacity, M_P (Z_gF_y) (or lower if compression flange or web limit states control) (b) Calculate the factored net-section fracture moment, M_{fnf} =$0.85Z_nF_u$. If $M_P \leq M_{fnf}$, the effects of holes (or fastener holes) shall be ignored and the flexural member shall be designed for its gross-section plastic moment as usually followed in the design solid beams. Otherwise, design the member to carry the factored net-section fracture moment.

Overall, the design moments calculated as per the proposed design approach resulted in higher design moments than that permitted by the current code provisions for flexural members having either flange holes or flange fastener holes. The 15% exemption rule, which is still in use as per the current CAN/CSA-S16.01 (Clause 14.1) code provision [1], is conservative for currently used structural steels which often possess a yield-to-ultimate strength ratio of less than 0.85. Note that the design moment as per the proposed design procedure in this investigation has a reduction factor of approximately 0.85 as compared to the maximum measured moments associated with the net-section observed in this investigation. Moreover, the suggested design method was analogous to the tension member provision as per the current CAN/CSA-S16.01 (Clause 13.2) code provision [1] eliminating unnecessary ambiguity in regards to the design of flexural members having holes (or fastener holes) in tension flanges. That is, the clause: 14.1 of the current CAN/CSA-S16.01 standard [1] treats the effects of holes and the effects fastener holes in different manner, in which when holes occur in flanges a theoretical net-section calculations shall be followed whereas, when fastener holes in beams is considered, the 15% exemption rule would be applied. However, the proposed method in this investigation follows a unified approach, in which the effects of holes or fastener holes that may present in flanges of a flexural member or a tension member would be treated in an identical manner. In addition, the proposed method as opposed to the current CSA code provision [1] takes into account the material characteristics in terms of yield-to-ultimate strength ratio.

5 CONCLUSIONS

The following points summarize the main observations of this research program:

[a] Experiments considered ASTM A992 steel with the measured yield-to-ultimate strength ratio of 0.77 beams having flange holes as high as 48% of the gross area of the tension flange. Though tension flange rupture was observed in some cases, the peak moments in all of the beams were higher than the gross-section plastic moment (M_P) for the beam [b]The strain measurements indicated that no great deviation occurred with regards to the position of the neutral axis of the gross cross-section when holes when holes were made in the tension flange only (or fastener holes occurred in both flanges) [c]The strain measurements made in the vicinity of hole region of beam specimens A75-3 and A75-2, in which holes existed in tension flanges only, were about 1.2% and 2%, respectively when the beam members reached the gross-section plastic moment, M_P. This yielded a conclusion that the flexural members with holes in tension flanges only require a strain in the range of 6-10 times the yield strain (0.2%) for the ASTM A992 steel as has been already verified by Dexter et al.[5] who performed flexural tests made of HPS 480W steel grade. [d]When holes were present in the tension flange only, and for the cases of fastener holes in both the tension flange and the compression flange, the failure of flexural members having the $A_{fn}F_u/A_{fg}F_y \geq 1.0$ was primarily due to lateral torsional buckling which was eventually followed by local buckling in the critical span (mid-span) region. It was noted in such cases that the gross-section plastic moment-to-the net-section fracture moment (M_P/M_{fn}) ratio was less than 0.85. [e] The design moment calculation as per the proposed design method was quite comparable with the present AISC code

provision [4]. However, beyond a threshold value, depending on the yield-to-ultimate strength ratio, the proposed method allowed higher moments on net-sections than the presently used design code provisions. It should also be noted that the proposed design moments are lower than the experimentally measured maximum moments on the net-section. Therefore, the design moments as per the proposed design method would be safe. [f] The ratio of the nominal net-section fracture strength ($A_{fn}F_u$)-to-the gross-section yield strength ($A_{fg}F_y$) did not seem to be as of a significant parameter for flexural members as it is for the tension members in determining the required strength since the flexural member (A50-1) having the $A_{fn}F_u/A_{fg}F_u$ ratio as low as 0.67 attained the maximum net-section moment which is more than the gross-section plastic moment. However, this parameter seemed to significantly influence the available total rotational capacity of flexural members having flange holes and fastener holes. [g] All beam specimens tested in this investigation attained more than the required rotation capacity of 3 before the onset of local buckling However, the required rotation capacity for non-seismic applications as per the current AISC specification [4] is greater than or equal to 7-9. In this investigation, beam specimens having the $A_{fn}F_u/A_{fg}F_u \geq 1.0$ exhibited substantial inelastic rotation capacity beyond the maximum load and were able to reach the gross-section plastic moment on the unloading branch. Thus, beam specimens with holes in the tension flanges only and fastener holes in both flanges satisfying $A_{fn}F_u/A_{fg}F_u \geq 1.0$ exhibited a total available rotation capacity, R_y of more than 9. If the condition was violated, the beam specimens failed primarily due to a rupture of tension flange through the flange holes which occurred before the flexural members reached the gross-section plastic moment again on the unloading branch. That is, for flexural members having the $A_{fn}F_u/A_{fg}F_u<1.0$ in the tension flanges, the inelastic deformation beyond the ultimate load was substantially reduced. However, the beam specimens with holes in both flanges satisfying the $A_{fn}F_u/A_{fg}F_u \geq 0.95$ exhibited a total available rotation capacity, R_y of more than 9. It should be noted that the available rotation capacities would substantially vary depending on many parameters, such as the cross-sectional geometry of the beam specimens, bracing locations (closer bracing will result in higher rotation ductility), material strain hardening, local instabilities associated with flange and/or web buckling, presence of initial geometric imperfections, etc. Thus, the generalization of available rotation ductility from a certain type of flexural test is not reasonable. Further details of this investigation are available in the thesis by Arasaratnam [6].

REFERENCES

[1] CSA (2003), Limit States Design of Steel Structures, CAN/CSA-S16-01, Canadian Standard Association, ON, Canada.

[2] Lilly, S.B., and Carpenter, S. T., (1940), Effective Moment of Inertia of a Riveted Plate Girder, Transactions, American Society of Civil Engineers, Paper No. 2089, pp.1462-1517.

[3] AISC (1989). Allowable Stress Design for Structural Steel Buildings,9th Edition, American Institute of Steel Construction, Inc., Chicago, Illinois, USA.

[4] AISC (2005). Load and Resistance Factor Design Specification for Structural Steel Buildings, 4th Edition, American Institute of Steel Construction, Inc., Chicago, Illinois, USA.

[5] Dexter, R.J. Alttstadt, A. and Gardner, C.A. (2002). Strength and Ductility of HPS70W Tension Members and Tension Flanges With Holes, Research Report, University of Minnesota, Minneapolis, MN, 55455-0116, USA.

[6] Arasaratnam, P. (2008), “Effects of Flange Holes on Flexural Behavior of Steel Beams”, Ph.D. Thesis, McMaster University, Hamilton, Ontario, Canada, p.xxv, p. 350.